AIChE WILEY InterScience DISCOVER SOMETHING GREAT

BIOENGINEERING, FOOD, AND NATURAL PRODUCTS

Precipitation of Soy Proteins: Particle Formation and Protein Separation

D. Y. M. Lui, J. D. Litster, and E. T. White
Division of Chemical Engineering, School of Engineering, The University of Queensland, Qld 4072, Australia

DOI 10.1002/aic.11070
Published online January 3, 2007 in Wiley InterScience (www.interscience.wiley.com).

The effect of pH on the precipitation of soy protein between pH 4 and 6.8 was investigated. Precipitation between pH 5.7 and 6.8 gave a binary liquid-liquid separation in which a protein-rich secondary liquid phase containing between 20 – 30 wt % protein of 80 – 99% purity in glycinin formed as droplets of 1 – 10 μm. The droplets could be coalesced upon centrifugation to form a homogeneous bottom liquid layer. The high-protein concentration phase was stable (did not precipitate or crystallize) for up to several months when stored at 4°C. Stable high-protein liquid phases have not previously been reported. In the pH region for which liquid-liquid separation occurred (pH 6.15 to 5.35), the droplet-size distribution was controlled by nucleation and growth. No drop breakage, and little or no drop coalescence was observed. Mixer speed and geometry did not have a large effect on the size of the protein-rich droplets in suspension. Nucleation occurred in two separate bursts at pH 6.15 and pH 5.85, followed by growth of the new nuclei as pH was decreased. Thus, the drop-size distribution was monomodal between 6.15 and 5.85, and bimodal between pH 5.85 and 5.35. At pH 5.6 and below, protein precipitated as amorphous material which intertwined with and bound primary particles into aggregates. These agglomerates grew with decreasing pH, particularly below pH 5.35, as more protein precipitated with amorphous material acting as a binder. The addition of NaCl prevented the liquid-liquid separation at higher pH. Instead solid precipitates of a different morphology were formed at low-pH only. *AIChE J,* 53: 514–522, 2007
Keywords: soy proteins, glycinin, β-conglycinin, precipitation, binary liquid-liquid separation

Introduction

Precipitation of soy proteins by acidification, to pH between 4 and 4.5, is a commonly used industrial method for producing soy proteins isolates, the most refined form of soy proteins available commercially. More recently, acid precipitation has also been used in schemes to separate the two naturally occurring soy protein groups glycinin (~360 kDa) and β-conglycinin (~180 kDa).[1–5] Separation occurs when an aqueous soy protein extract is acidified to between pH 5.5 and 6.5.

Understanding the particle formation during the precipitation process is important as it can influence the efficiency of the precipitation process, as well as subsequent downstream processes, such as the solid-liquid separation step, usually achieved by centrifugation. There are limited studies on the precipitation of soy protein between pH 5.5 and 6.5 as industrial interest in the separation of glycinin and β-conglycinin is relatively new. Most of the previous studies on soy protein precipitation are limited to precipitation at pH 4 to 5.[6–13] Precipitation of soy protein within this pH range is generally thought to occur by the rapid formation of primary particles

Correspondence concerning this article should be addressed to J. Litster at j.litster@cheque.uq.edu.au.

in the size range of 0.1 – 0.3 μm followed by aggregation of these particles via collision to aggregates of size about 1 – 50 μm. The formation of the primary particles occurs on a timescale much shorter than that of the overall precipitation process. Precipitation at other pH levels is likely to produce particles of different morphology.

It has been reported that a high protein concentration secondary liquid-phase forms when the aqueous protein extract was acidified to between pH 6.8 and 5.7.[14] This phenomenon has not been widely appreciated in the literature. It is, however, highly significant as it presents a unique opportunity for new product development, allowing food manufacturers to incorporate liquid soy protein into food formulations, where it has previously been difficult with solid protein precipitates.

In this article, particle formation during the precipitation of soy proteins is studied over a range of pH from 4 to 6.8. Partitioning of the main soy protein components between the phases, and the dispersed phase properties (liquid or solid, protein content, particle-size distribution, density and viscosity) are reported. Particle formation and growth mechanisms are examined in detail and implications for industrial processing and new product development are discussed. The solubility of soy proteins in aqueous solutions at various pH has been discussed elsewhere.[15]

Materials and Methods

Preparation of the protein secondary-liquid phase

An aqueous-protein extract was first prepared by mixing 1 part defatted soy flour (Cargill Oilseeds Processing, U.S.A.) with 10 parts alkaline water (containing 15 mM added $Na_2S_2O_5$, with pH adjusted to 8.5 by NaOH), usually in a 1 L volume vessel. The suspension was stirred with an overhead impeller in a constant temperature water bath at 21°C for 1 h. The aqueous-protein extract was recovered by centrifuging for 30 min at 9,600 g. The aqueous protein extract was then acidified to between pH 6.8 and 5.7 with 1 M HCl, whereupon the highly viscous secondary protein-rich liquid phase droplets were formed. The secondary phase was recovered by centrifuging at 9,600 g for 30 min. The low-viscosity supernatant phase was decanted off. Further details are given elsewhere.[15]

Determination of Protein Phase Properties

Protein content was determined by UV spectrophotometry (absorbance at 280 nm, E = 1.913 $cm^{-1}(mg/mL)^{-1}$). Fractional composition of the protein was determined by sodium dodecyl sulfate — polyacrylamide gel electrophoresis (SDS-PAGE) followed by gel density image analysis. Prior to analysis, the highly viscous secondary phase was dissolved in known amounts of 0.1 M NaOH.

Viscosity measurements of the protein-rich liquid phase were made with a Haake RheoScope 1 Optical Rheometer (Thermo Haake, Germany) controlled with the Haake RheoWin software. A cone and plate sensor with cone diameter of 60 mm, cone angle of 1° and gap width of 0.026 mm was used. Temperature was kept constant at 21°C. The rheometer was operated in strain controlled mode between 0.1 and 100 s^{-1}.

The densities of the low-viscosity fluids (the aqueous extract and the supernatant phase) were measured with a 10 mL specific gravity bottle with a capillary cap. Slightly cooled samples were put into the specific gravity bottle, and placed into a constant temperature bath at 22°C to allow for slight expansion to ensure the capillary cap was completely filled. The bottle was calibrated with water and repeated measurements showed that the 95% confidence interval error of the method results was less than 0.05%.

The density of the protein-rich phase was measured by the Archimedes' Principle where the buoyant force on a submerged object is equal to the weight of the fluid that is displaced by the object. The specific gravity bottle was not used as high-viscosity fluids tended to block the capillary. Repeated measurements showed that the 95% confidence interval error of the Archimedes' method was less than 0.5%.

Precipitation Experiments

The aqueous protein solution was acidified to a range of pH levels (6.8 to 4.0). The solution was stirred at 450 rpm with a four-blade 45° axial-flow impeller (D = 58 mm), in a 300 mL beaker (D = 70 mm; H = 100 mm), with the impeller set 25 mm off the bottom of the beaker. Acid (1 M HCl) was added while stirring at a constant speed.

The particle-size distribution of the suspension was measured using the Malvern Mastersizer/E. Particle-size measurements could not be made for suspensions at pH greater than 6.2, as the concentrations of particles were too low. Periodic samples up to 15 min were taken at constant pH to determine if there were any changes in the particle-size distribution over time. Time zero was when the solution had reached the desired pH with the addition of HCl. Pictures of the precipitates were taken to observe precipitate morphology with an Olympus BX40 optical microscope.

The experiments were repeated with solutions containing 0.2 M and 0.5 M of additional NaCl to determine the effect of salt on the precipitate formation. However, due to the increased protein solubility with the addition of salt[15] which resulted in a decrease in the particle concentration in the suspension, particle-size distribution measurements could not be accurately made of suspensions at pH greater than 5 for the 0.2 M NaCl solution and pH greater than 4 for the 0.5 M NaCl solution.

To determine the effect of mixing speed on droplet breakage and/or coalescence of the secondary protein-rich liquid phase, the solution was stirred with a four-blade 45° axial flow impeller (D = 58 mm) in a 300 mL beaker (D = 70 mm; H = 100 mm) with the impeller set 25 mm off the bottom of the beaker, while 1M HCl was added to bring the solution to pH 6.2. Stirring initially was at either high-speed (450 rpm) or low-speed (200 rpm). Samples were taken periodically to determine any change in the droplet-size distribution with time using the Malvern Mastersizer/E. Time-zero was when the solution had reached the desired pH. The first sample was taken as soon as possible thereafter (ca. 6 s). When the droplet-size distribution appeared to become constant after a period of time, the stirrer speed was reduced from high-speed to low-speed (for the "speed-down" experiment), or increased from low speed to high speed (for the "speedup" experiment). Further samples were then taken

periodically to determine any change in the droplet-size distribution. The experiments were repeated with a magnetic stirrer (L = 39 mm; D = 8 mm) on the beaker bottom for comparison.

Results

High protein concentration secondary liquid phase

A high protein concentration secondary liquid phase was formed when the aqueous protein extract was acidified to between pH 6.8 and 5.7. The protein-rich phase appeared as spherical droplets between 1 – 10 μm in size, as shown in Figure 1a. Upon centrifugation, the droplets coalesced to form a highly viscous bottom phase. The phase diagram (composition of protein in each phase at a given pH) for the liquid-liquid separation is shown in Figure 2. As the protein-rich phase had to be redissolved in NaOH for protein content measurement, these data were subjected to larger experimental errors. Mass balance calculations were, therefore, made as a check, and these are also plotted in Figure 2. Note the log scale for protein concentration.

The protein content of the supernatant phase was between 2 and 3 wt %. The protein content of the secondary phase was between 20 and 30 wt %, 10 times that of the supernatant phase. The protein yield of the protein-rich phase (fraction of extract total protein in phase) is shown in Figure 3. Between 10 and 50% of the total protein was recovered in the liquid phase between pH 6.8 and 5.7.

The β-conglycinin and glycinin composition of the secondary phase is shown in Figure 4. Between 1 to 3% of the phase consisted of a mixture of other minor proteins, and, therefore, the β-conglycinin and glycinin composition do not added up to exactly 100%. The secondary liquid phase is predominantly glycinin, and significant fractionation has occurred. The glycinin purity of the separated phase is plotted against glycinin yield in Figure 5.

The densities of the protein extract, the supernatant phase and the protein-rich secondary liquid phase were measured and plotted against their, respectively protein concentrations in Figure 6. As expected, density increased with increasing protein concentration.

The viscosity of the secondary liquid phase was measured and the results are shown in Figure 7. The sample was tested in strain-controlled mode with strain rates of 0.1 to 100 s^{-1} in an up-hold-down sequence as shown in Figure 7a. The shear stress results show that the secondary phase was slightly shear-thinning with a viscosity (apparent viscosity) of between 5 to 10 Pa.s, that is, of order 10,000 times that of water. Interestingly, the shear stress response to decreasing strain rate was not identical with that of increasing strain rate, indicating that there were probably some shear-induced structural changes within the phase. This may be of some importance in the industrial application of the material.

Effect of pH on percipitate size and morphology

The morphology and size distribution of the precipitated phase changes dramatically as pH is decreased. This is clearly shown in the micrographs (Figure 1) and in the particle-size distributions (Figure 8). In the pH range 6.15 to 5.85, monomodal distributions of a protein-rich secondary phase were formed. Interestingly, the particle size distribution between pH 5.8 and 5.35 were bimodal with one peak at approximately 2 μm, and another at approximately 10 μm. Pictures of the particles formed at pH 5.85 and 5.7 (Figure 1b and c) show that the particles were spherical droplets and that there were small particles present, as well as large particles, confirming that the distributions were indeed bimodal, and the result not an artifact of the measurements. Figure 1d shows the onset of amorphous precipitation between pH 5.6 and 5.35. The amorphous material intertwined with and bound the spherical droplets causing aggregation. The size of the particles continued to increase at pH below 5.3 as the aggregates were increasingly bound by the amorphous precipitate. The median particle size was up to 30 μm at pH 4. Figure 1f shows the agglomerate morphology of the particles in this pH range. A solid plug rather than a viscous liquid resulted upon centrifugation of this low-pH level phase. It is unclear whether the spherical particles in Figure 1e remained liquid, or were transformed to solid precipitate. It is possible these aggregates were a combination of liquid, gel and solid phases.

The volume median particle size (d_{50}), and also the mode size are plotted vs. pH in Figure 9. The data at each pH are the average between three measurements taken over 15 min. The modes for the smaller peak of the bimodal distributions are also plotted in Figure 9. Precipitation occurred rapidly and there was in fact very little change in the size distribution with mixing time after acid addition.

Effect of mixing speed on the droplet-size distribution

The effect of mixing conditions on the drop-size distribution was studied at pH 6.2 with no added salt, that is, conditions which yielded liquid-liquid phase separation. Experiments were conducted with a four-blade axial turbine impeller. The volume median droplet sizes (d_{50}) for the overhead impeller "speed-down" and "speed-up" experiments are shown in Figure 10. There was a slight increase in the median droplet size from 2.7 to 3.5 μm, with time prior to the changes in the speed. However, the magnitude of the increase was close to the error of the measurements. No significant change in the droplet size was found with or after the speed change.

An estimate on the number of droplets per kg of suspension (with size greater than 0.65 μm, a convenient size minimum) was calculated from the volume-based size distribution, density of the droplets and the droplet concentration. There was a small, but probably not significant, decrease over time in the number of droplets from 3.1×10^{12} to 1.8×10^{12} for the "speed-up" experiment, prior to the speed change. No significant change in the number of droplets was observed for the "speed-down" experiment. The experiments were repeated with a bottom located magnetic stirrer for comparison. The droplet sizes of the "speed-up" experiment ($\sim$3.8 μm) were slightly larger than those of the "speed-down" experiment ($\sim$3.2 μm). There was a smaller number of droplets in the "speed-up" experiment as the droplets were larger. The number of droplets for the "speed-down" experiment decreased from 4.1×10^{12} to 3.1×10^{12} as the speed changed. These changes are not large.

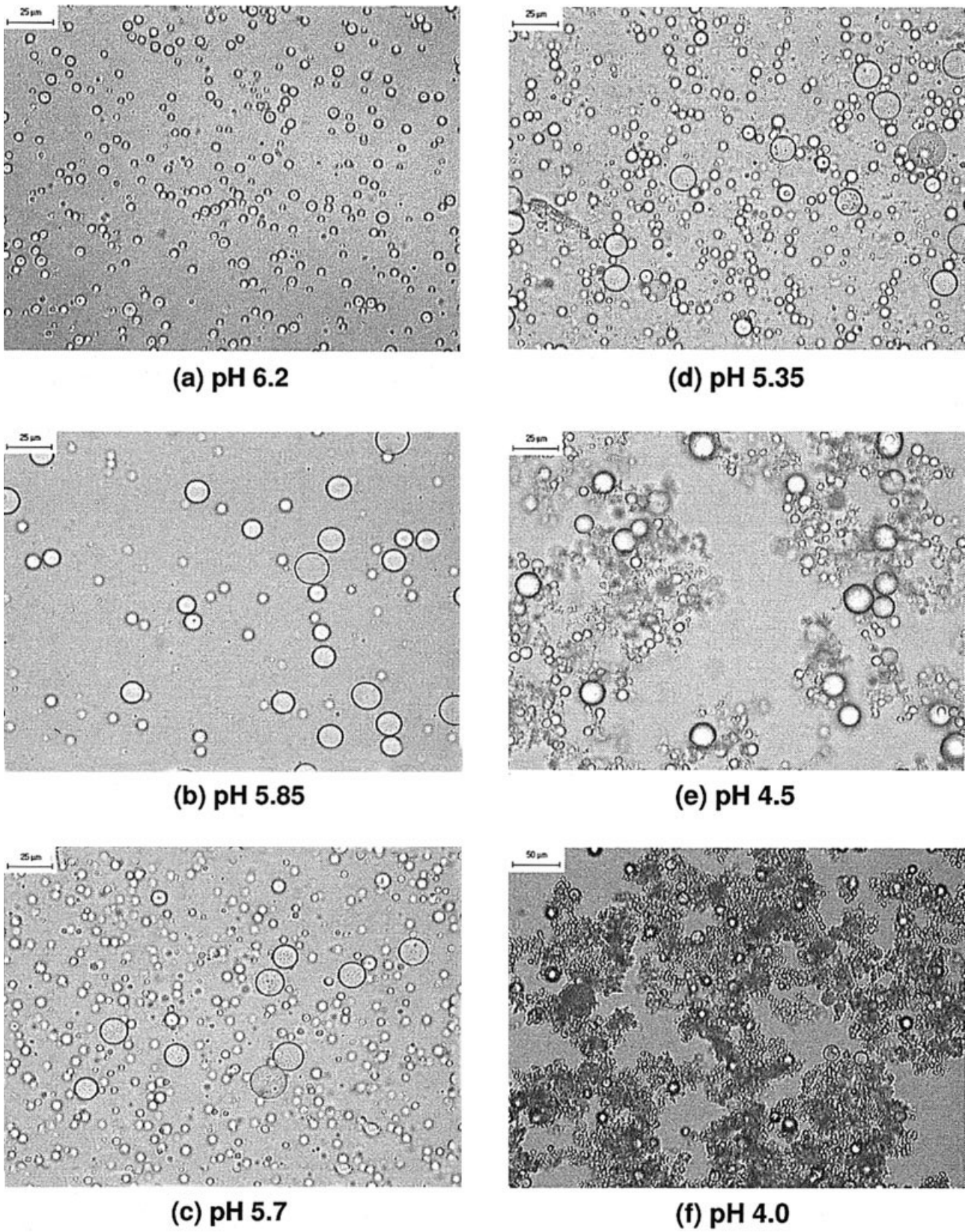

Figure 1. Photographs of precipitate morphology with changing pH in the range 6.15 to 4.0 (no added NaCl, T = 21°C).

Scale bar =25 μm for (a) to (e) and 50 μm for (f).

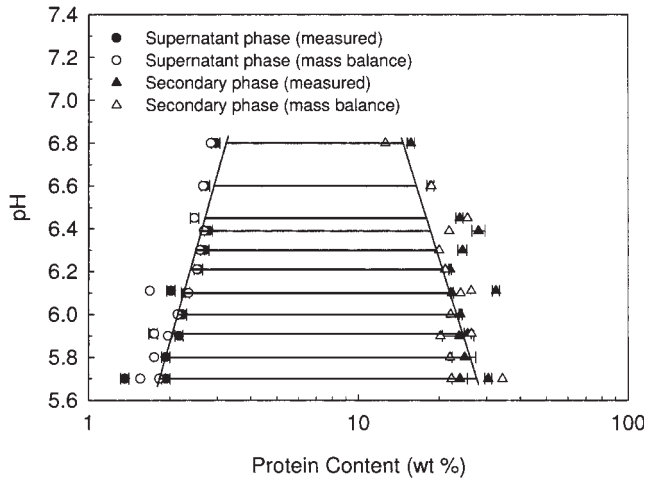

Figure 2. Liquid-liquid separation phase diagram, 21°C.

Thus, the mixing method and intensity does not appear to have a great effect on the droplet sizes. These results also confirm that precipitation is fast with little change in the drop-size distribution, with time in all experiments.

Effect of salt concentration on precipitation

The volume median sizes of the particles when salt was added to the solution are shown in Figure 11. Data for no added salt are plotted here for comparison. Particle-size measurements could not be made at higher pH levels as the particle concentration was too low. The particle concentration with added NaCl was much lower than with no added NaCl, due to the increased solubility with increased salt concentrations.[15]

The agglomerated morphology of the particles precipitated with added salt is shown in Figures 12 and 13. When salt was present in the solution, the precipitates appeared as small amorphous particles and no liquid-liquid separation occurred at any pH. No droplets were found and upon centrifugation the bottom layer was a solid plug rather than a viscous liquid layer.

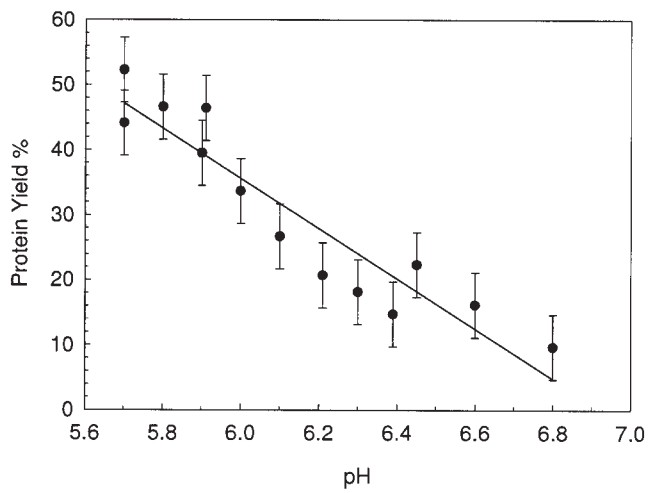

Figure 3. Protein yield of the protein-rich liquid phase.

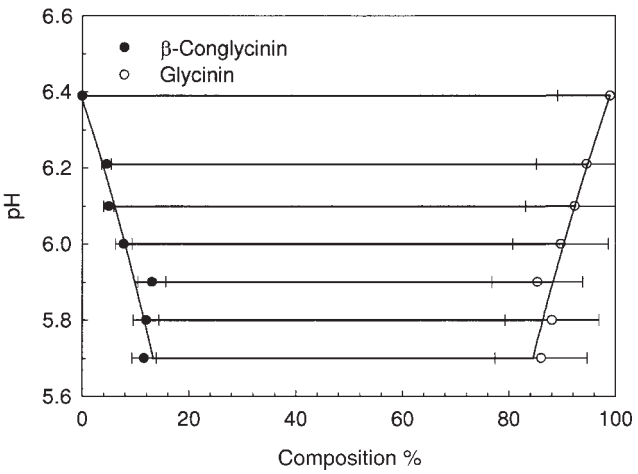

Figure 4. *β*-conglycinin and glycinin composition of the secondary liquid phase.

Composition as % of total protein; 95% error bars are shown.

Discussion

High protein concentration secondary liquid phase

The protein-rich liquid phase formed between pH 6.8 to 5.7. Coincidentally, these were the conditions under which, for these extracts, separation of glycinin and *β*-conglycinin occurred. This behavior is interesting as the only other report of the liquid-liquid separation phenomena for soy proteins in the literature was by Bogracheva et al.[14] where liquid-liquid separation occurred between pH 6 and 6.6. Other studies of glycinin and *β*-conglycinin separation at similar conditions did not report the occurrence of a secondary liquid phase.[1–5]

Similar binary liquid-liquid separation in other protein solutions have been reported.[16–20] The secondary liquid phases observed in the literature were generally found to be a metastable phase and eventually crystallized or precipitated. However, for the soy proteins, the secondary liquid phase did not crystallize or precipitate for up to several months when the secondary phase was stored at 4°C with or without the supernatant phase. This presents a unique opportunity for new prod-

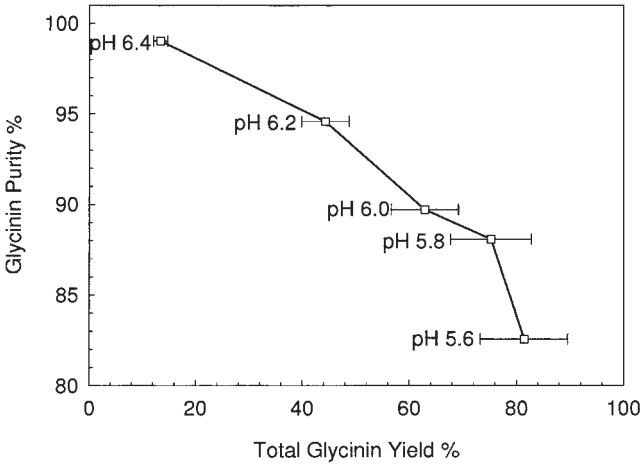

Figure 5. Glycinin purity vs glycinin yield for the secondary liquid phase at 21°C (pH 6.4 – 5.6).

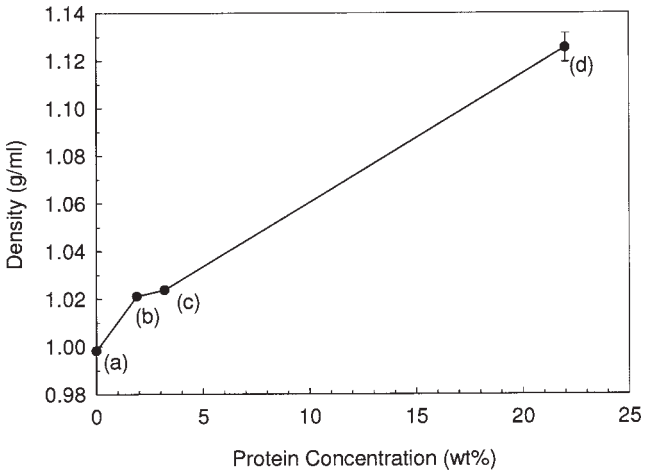

Figure 6. Density of soy protein solutions and secondary liquid phase at 22°C. (a) water, (b) supernatant phase at pH 6.2, (c) 10:1 aqueous protein extract, and (d) secondary liquid phase at pH 6.2.

uct development. Stable high-protein liquids have not previously been reported.

At high pH, only a small amount of protein was partitioned into the secondary phase, thus, the amount of protein in the secondary phase was low, while the amount of protein in the supernatant phase was high. As pH is lowered, more protein was partitioned into the secondary phase, and the amount of protein in the secondary phase increased. Accordingly, the protein yield of the protein-rich liquid phase increases with decreasing pH. This is confirmed in Figure 3, which shows the increasing protein yield of the protein-rich phase with decreasing pH. Up to 50% of the total protein in the original aqueous extract was recovered in the protein-rich phase at pH 5.7.

The secondary liquid phase was purest in glycinin at the higher pH (see Figure 4). As pH was lowered, some β-conglycinin was also partitioned into the secondary phase, thus, purity was decreased. Even at pH 5.7, the secondary phase was 80% pure in glycinin, hence precipitation at these pH levels can effectively separate glycinin from β-conglycinin.

High-concentration liquid soy protein presents a unique opportunity for new product development. It may allow food manufacturers to incorporate soy protein into food formulations, where it has previously been difficult with solid protein precipitates. These novel products include ready-to-drink smoothies, meal replacements, yogurts and ice-creams offering the health benefits of soy protein. Formulating these products with protein precipitates often caused settling issues in the manufacturing process, as well as in the final product. Undissolved precipitates in the final product also led to an undesirable "gritty" mouth-feel. The use of the liquid soy protein may alleviate these problems. Further studies into the behavior of the liquid protein in individual formulations, however, would be required for successful incorporation.

Drop formation and growth mechanisms

In the operating region where liquid-liquid separation occurs, the main mechanisms that control the droplet-size distribution are nucleation and growth, rather than coalescence and breakage of drops.

As pH is decreased from pH 6.15 to pH 5.8, the d_{50} of the droplets increased from 3.5 μm to 7.5 μm, while there was no significant change in the number of droplets. This is consistent with a nucleation burst at pH 6.15 followed by droplet growth as protein was transferred from the supernatant to the existing droplets. The increase in drop size is consistent with the total volume of secondary liquid phase formed over this pH range.

The lack of any effect of mixing conditions on drop size distribution in this pH range supports the proposed drop formation mechanism. Drop breakup in simple shear flow is unlikely at viscosity ratios of above 4.[21] The apparent viscosities of the secondary liquid phases were found to be between 5 to 10 Pa.s (with a density about 1.125 g/mL). The viscosity ratio of the discrete to continuous phases is of order 10,000, and, therefore, breakup of the droplets would not be expected to occur.

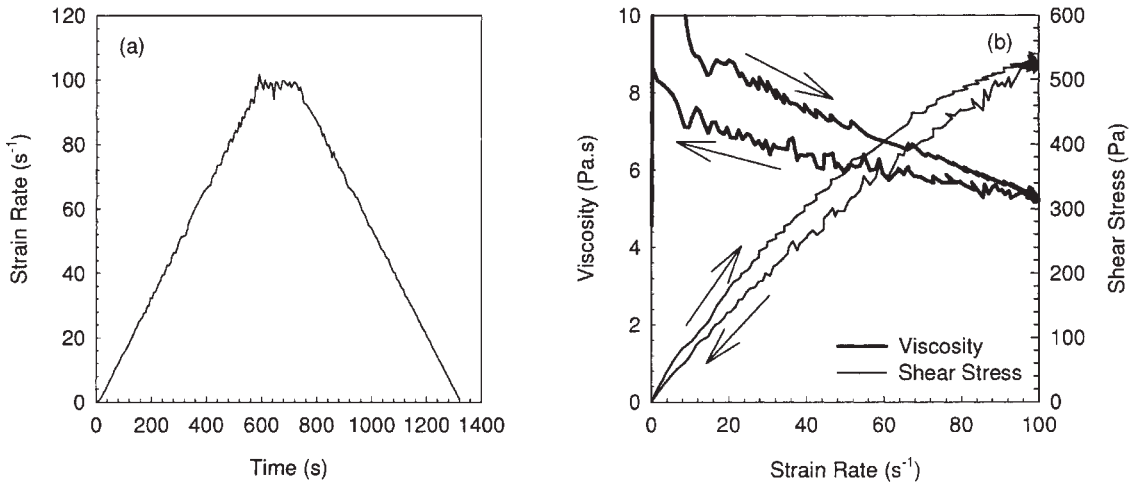

Figure 7. Rheology of the secondary liquid phase at 21°C (a) Strain rate applied, and (b) Shear stress and viscosity in response to applied strain.

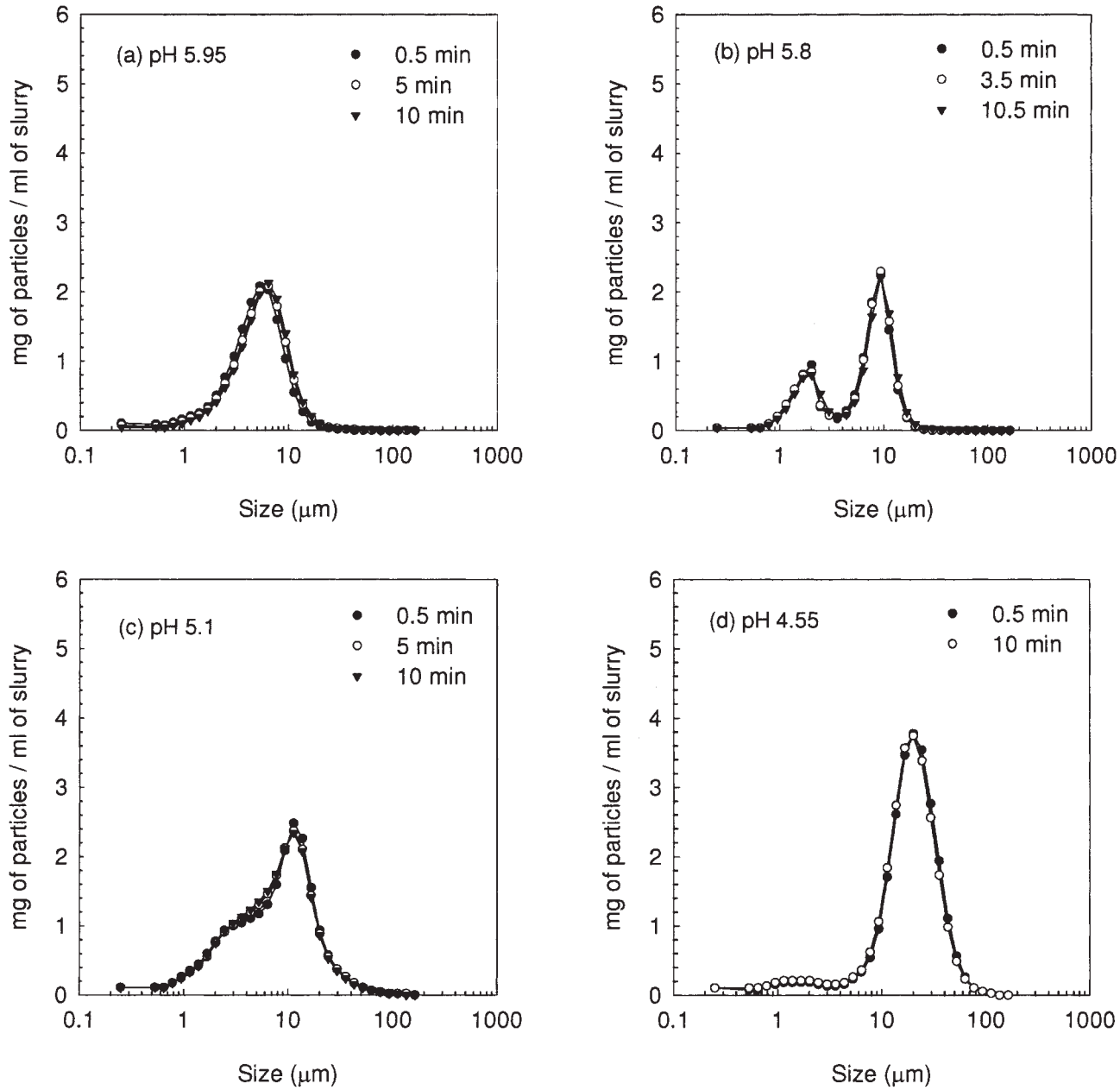

Figure 8. Precipitate-size distributions as a function of changing pH. (21°C, no added NaCl).

Over the range of mixing speeds studied, mixer speed and stirrer geometry did not have a large effect on the droplet size distribution. The median droplet size under all of the shear condition studied was between 2.5 to 4 μm. There was some evidence to suggest that a small amount of droplets coalesced under these mixing speeds, but no drop breakup occured. Overall, the drop size distribution in the range pH 6.15 to pH 5.8 is primarily controlled by a nucleation burst followed by growth of the nucleated droplets.

At pH 5.8, there is a second nucleation burst which causes the formation of a bimodal size distribution. This second burst is followed by further growth of the new drops as pH is reduced to 5.35 with a shift in the second mode from 1.7 to 3.5 μm. At the same time, there is no further growth of the existing drops formed at pH > 5.8, and the size of these drops is unchanged. The second nucleation burst results in an increase in the number of drops at pH 5.8. These results were unexpected, and the reason for the secondary nucleation burst is unclear.

Between pH 5.6 and 5.35, small amounts of an amorphous material precipitated which intertwined with and bound the spherical droplets causing limited aggregation. It was not clear whether the amorphous material was a solid or a gel phase. It is possible that it was a combination of both. At pH below 5.35, serious agglomeration of the primary particles was observed, and this dominated the size distribution and morphology of the particulate product. The precipitates were increasingly bound by the additional amorphous material being precipitated. Hence the size of the agglomerates increased and their numbers decreased. It was unclear whether the spherical

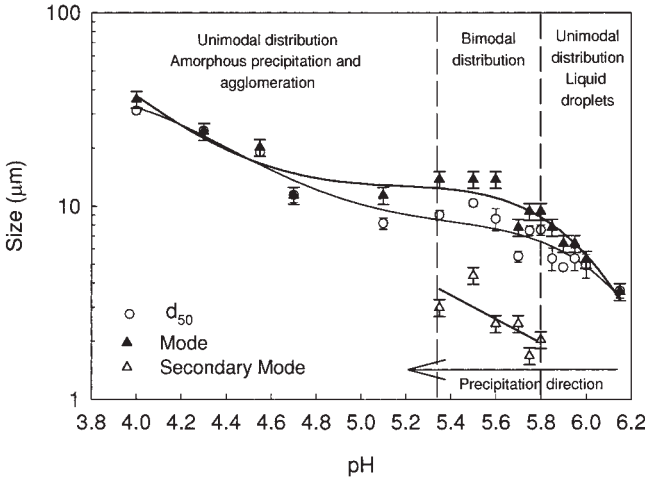

Figure 9. Effect of pH on volume median and mode sizes.

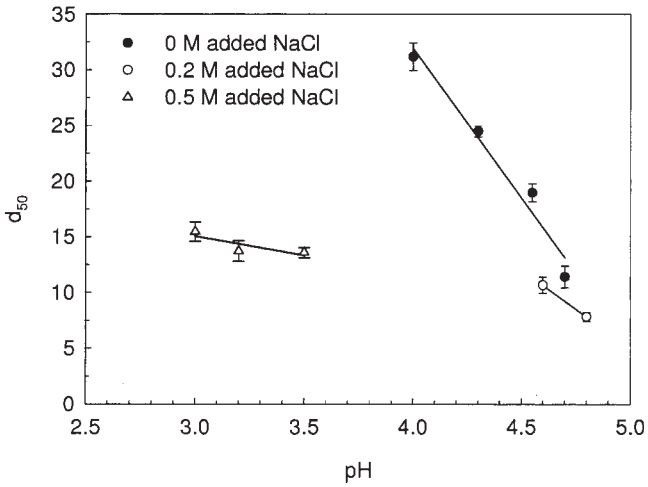

Figure 11. Volume median particle size for runs with added NaCl.

particles in Figure 1e remained liquid or transformed to a solid precipitate. It is possible that these aggregates were a combination of liquid, gel and solid phases.

Effect of salt concentration on precipitation

The protein precipitates with 0.2 M and 0.5 M added NaCl were smaller than the no added NaCl protein precipitates. There was a possible increase in size with decreasing pH for both 0.2 M and 0.5 M added NaCl (Figure 11). The number of particles in suspension decreased with decreasing pH indicating that the precipitate size increased via agglomeration. The number of particles in the 0.5 M added NaCl suspension was much lower than for the 0.2 M added NaCl suspension. This was because the particle concentration was lower, and the agglomerates were larger.

The morphology of the precipitates with added salt was different to those with no added salt. Aggregation of primary particles occurred, but there was no clear evidence of the appearance of material acting as a binder. The salting-in effect on soy protein may also lead to different types of molecular interactions that affect the morphology of the precipitates.

Conclusions

Precipitation of soy proteins between pH 5.7 and 6.8 gave a binary liquid-liquid separation in which a protein-rich secondary liquid phase containing between 20 – 30 wt % protein of 80 – 99% purity in glycinin formed as droplets of 1 – 10 μm. The droplets could be coalesced upon centrifugation to form a homogeneous bottom liquid layer. The high-protein concentration phase was stable (did not precipitate or crystallize) for up to several months when stored at 4°C.

In the pH region for which liquid-liquid separation occurred (pH 6.15 to 5.35), the droplet-size distribution was controlled by nucleation and growth. No-drop breakage, and little or no-drop coalescence was observed. Mixer speed and geometry did not have a large effect on the size of the protein-rich droplets in suspension. Nucleation occurred in two

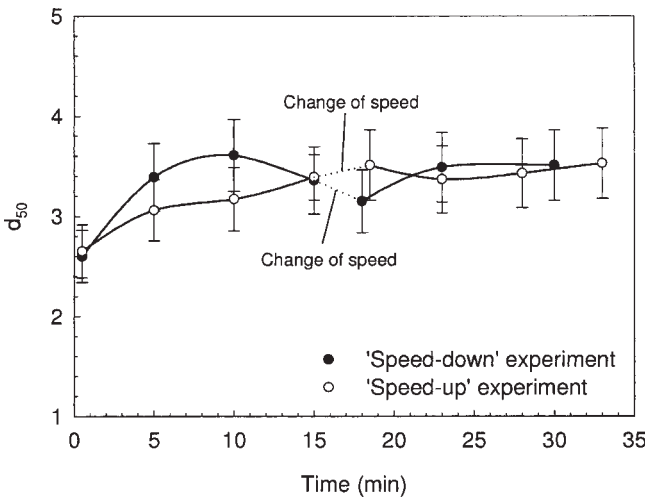

Figure 10. Volume median droplet sizes for runs with axial turbine impeller.

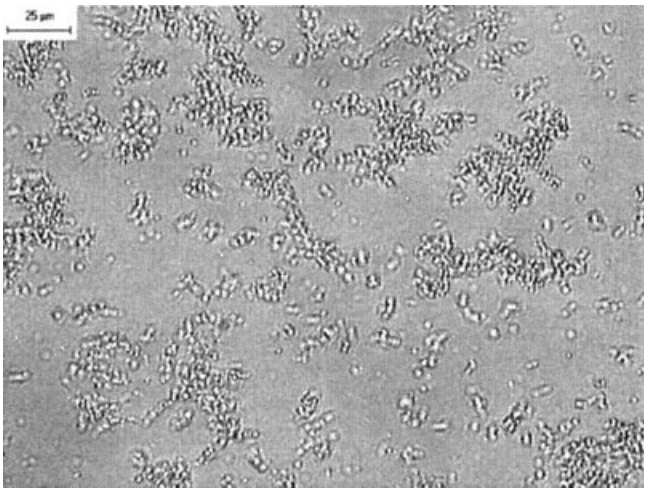

Figure 12. Example of amorphous precipitates for runs with 0.2M added NaCl pH 4.8, calibration bar = 25 μm.

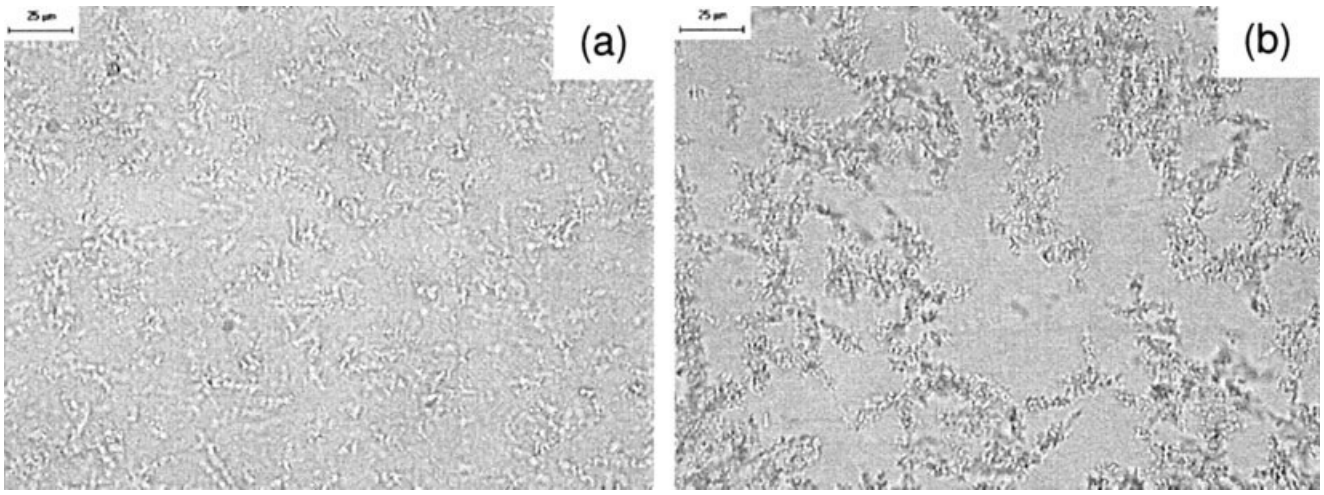

Figure 13. Examples of amorphous precipitates for runs with 0.5 M added NaCl (a) pH 4.5; (b) pH 3.5; calibration bar = 25 μm.

separate bursts at pH 6.15 and pH 5.85, followed by growth of the new nuclei as pH was decreased. At pH 5.6 and below, protein precipitated as amorphous material which intertwined with and bound primary particles into aggregates. These agglomerates grew with decreasing pH, particularly below pH 5.35, as more protein precipitated with amorphous material acting as a binder. The addition of NaCl prevented the liquid-liquid separation at higher pH.

Literature Cited

1. Howard PA, Lehnhardt WF, Orthoefer FT; A. E. Staley Manufacturing Company, assignee. 7S and 11S Vegetable Protein Fractionation and Isolation. U.S. patent January 11; 1983;4,368,151.
2. Nagano T, Hirotsuka M, Mori H, Kohyama K, Nishinari K. Dynamic viscoelastic study on the gelation of 7s globulin from soybeans. *J of Agricultural and Food Chemistry*. 1992;40.
3. Thanh VH, Shibasaki K. Major proteins of soybean seeds. A straightforward fractionation and their characterization. *J of Agricultural and Food Chemistry*. 1976;24:1117–1121.
4. Wu S, Murphy PA, Johnson LA, Fratzke AR, Reuber MA. Pilot-plant fractionation of soybean glycinin and beta-conglycinin. *J of the A Oil Chemists Soc*. 1999;76(3):285–293.
5. Wu S, Murphy PA, Johnson LA, Reuber MA, Fratzke AR. Simplified process for soybean glycinin and beta-conglycinin fractionation. *J of Agricultural and Food Chemistry*. 2000;48:2702–2708.
6. Bell DJ, Dunnill P. The influence of precipitation reactor configuration on the centrifugal recovery of isoelectric soya protein precipitate. *Biotechnol and Bioeng*. 1982;24:2319–2336.
7. Bell DJ, Dunnill P. Shear disruption of soya protein precipitate particles and the effect of aging in a stirred tank. *Biotechnol and Bioeng*. 1982;24:1271–1285.
8. Glatz CE, Hoare M, Landa-Vertiz J. The formation and growth of protein precipitates in a continuous stirred-tank reactor. *AIChE J*. 1986;32(7):1196–1204.
9. Grabenbauer GC, Glatz CE. Protein precipitation — Analysis of particle size distribution and kinetics. *Chem Eng Communication*. 1981; 12:203–219.
10. Nelson CD, Glatz CE. Primary particle formation in protein precipitation. *Biotechnol and Bioeng*. 1985;27:1434–1444.
11. Petenate AM, Glatz CE. Isoelectric precipitation of soy protein: I. Factors affecting particle size distribution. *Biotechnol and Bioeng*. 1983;25(12):3049–3058.
12. Petenate AM, Glatz CE. Isoelectric precipitation of soy protein: II. Kinetics of protein aggregate growth and breakage. *Biotechnol and Bioeng*. 1983;25(12):3059–3078.
13. Virkar PD, Hoare M, Chan MYY, Dunnill P. Kinetics of the acid precipitation of soya protein in a continuous-flow tubular reactor. *Biotechnol and Bioeng*. 1982;24:871–887.
14. Bogracheva TY, Bespalova NY, Leont'ev AL. Isolation of 11S and 7S globulins from seeds of glycine max. *Appl Biochem and Microbiology*. 1996;32(4):429–433.
15. Lui D. *Protein Separation by Precipitation for Glycinin and B-Conglycinin*. PhD Thesis, The University of Queensland; 2005.
16. Broide ML, Berland CR, Pande J, Ogun OO, Benedek GB. Binary-Liquid Phase Separation of Lens Protein Solutions. *Proceedings of the National Academy of Science, USA*. 1991;88:5660–5664.
17. Galkin O, Vekilov PG. Are nucleation kinetics of protein crystals similar to those of liquid droplets. *J of the A Chem Soc*. 2000;122: 156–163.
18. Galkin O, Vekilov PG. Nucleation of protein crystals: critical nuclei, phase behaviour, and conrol pathways. *J of Crystal Growth*. 2001; 232:63–76.
19. Muschol M, Rosenberger F. Liquid-liquid phase separation in supersaturated lysozyme solutions and associated precipitate formation/crystallization. *J of Chem Phys*. 1997;107(6):1953–1962.
20. Vekilov PG. Dense liquid precursor for the nucleation of ordered solid phases from solution. *Crystal Growth and Design*. 2004;4(4): 671–685.
21. De Bruijn RA. Deformation and breakup of drops in simple shear flows. Technische Universiteit Eindhoven; 1989. PhD Thesis.

Manuscript received July 31, 2006, and revision received Oct. 29, 2006.